Direct Measurements of Forces between Phosphatidylcholine and Phosphatidylethanolamine Bilayers in Aqueous Electrolyte Solutions

Johan Marra and Jacob Israelachvili*
Department of Applied Mathematics, Research School of Physical Sciences, Australian National University, Canberra, A.C.T. 2601, Australia
Received November 15, 1984

ABSTRACT: We report direct measurements of the full interbilayer force laws (force vs. distance) between bilayers of various phosphatidylcholines and phosphatidylethanolamine in aqueous solutions. Bilayers were first deposited on molecularly smooth (mica) surfaces and the interbilayer forces then measured at a resolution of 1 Å. Three types of forces were identified: attractive van der Waals forces, repulsive electrostatic (double-layer) forces, and (at short range) repulsive steric hydration forces. Double-layer forces, which arise from ion binding, were insignificant in monovalent salt solutions, e.g., NaCl up to 1 M, but were already present in solutions containing millimolar levels of $CaCl_2$ and $MgCl_2$, giving rise to forces in excellent agreement with theory. Ca^{2+} binds more strongly than Mg^{2+}, and both bind less to lecithin bilayers in the fluid state ($T > T_c$). The plane of charge coincides with the location of the negative phosphate groups, while the effective plane of origin of the van der Waals force is 4–5 Å farther out. In water, the adhesion energies are in the range 0.10–0.15 erg/cm^2 for lecithins and ~0.8 erg/cm^2 for phosphatidylethanolamine. The adhesion energies vary on addition of salt due to changes in the repulsive double-layer and hydration forces rather than to a change in the attractive van der Waals force. The short-range repulsive forces which balance the van der Waals force at separations of 10–30 Å are due to a combination of hydration and steric repulsions, the latter arising from thermal motions of head groups and thickness fluctuations of fluid bilayers (above T_c). It is also concluded that bilayer fusion is not simply related to the interbilayer force law.

A knowledge of the interaction forces between amphiphilic surfaces such as lipid bilayers and surfactant monolayers across water is necessary for understanding the properties of many colloidal and biological systems, e.g., the interactions between micelles, vesicles, microemulsion droplets, and surfactant-coated colloidal particles. Effective detergent action and the stability of soap films, foams, and liquid-crystalline surfactant phases are also ultimately dependent on these forces. In the more biological area, membrane–membrane and vesicle–membrane interactions underlie all phenomena involving intermembrane coupling such as adhesion, membrane stacking, and fusion. Even though many biological membranes contain 50% or more protein by weight, the role of lipids is unlikely to be purely passive, and it is almost certain that the total interaction between membranes is a cooperative process involving the concerted action of both lipids and proteins.

As regards the different interaction forces themselves, be they van der Waals, electrostatic, solvation (solvent structure induced), or steric forces, we may presume that the same *fundamental* forces are always operating, the lipids and proteins merely modulating their strength. It is these fundamental interactions that form the subject of this paper.

Hydration Forces. Taking into account only attractive van der Waals and repulsive electrostatic double-layer forces (Verwey & Overbeek, 1948), we expect that in the absence of any strong double-layer repulsion—as would arise for nonionic and zwitterionic head groups or in high salt for charged lipids—all surfaces should come into strong irreversible adhesive contact with no water remaining between them. That this does not occur is due to the existence of an additional strongly repulsive short-range (<3 nm) force, commonly referred to as a solvation force, a structural force, or a *hydration force*, which has now been found to occur in many systems. In particular, this force occurs between nonionic surfactant bilayers with poly(oxyethylene) head groups (I. G. Lyle and G. J. T. Tiddy, unpublished experiments), between zwitterionic lipid bilayers of phosphatidylcholine (PC)[1] and PE (Lis et al., 1982a), and between galactolipid bilayers of MGDG and DGDG (Marra, 1985). It is interesting that the latter four lipids are all uncharged at physiological pH, and yet they are the most abundant lipids in animal and plant membranes. Their highly hydrated head groups ensure that their bilayers and vesicles will not adhere strongly, let alone fuse, even under conditions where there is no repulsive double-layer force.

Repulsive hydration forces between two particles or surfaces arise whenever there are hydrated (hydrophilic) surface groups. As the two surfaces approach each other, the water between them must be removed to the bulk solution, which is energetically unfavorable and appears as a repulsive hydration—or more correctly a "dehydration"—force between them (Israelachvili, 1985a). The range of the repulsive hydration forces so far measured between amphiphilic (surfactant and lipid surfaces is 2–3.5 nm, below which the force rises steeply, dominating over the van der Waals and double-layer forces.

Three different experimental techniques have so far been used. The earliest involved soap films where the pressure across the aqueous layer was measured as a function of water layer thickness (Lyklema & Mysels, 1965; Clunie et al., 1967). The second method commonly used for measuring repulsive hydration forces involves measuring the osmotic or hydrostatic "swelling" pressures between aligned clay sheets in water (Van

[1] Abbreviations: PC, phosphatidylcholine (lecithin); PE, phosphatidylethanolamine; DLPC, dilauroylphosphatidylcholine; DMPC, dimyristoylphosphatidylcholine; DPPC, dipalmitoylphosphatidylcholine; DSPC, distearoylphosphatidylcholine; DPPE, dipalmitoylphosphatidylethanolamine; POPC, 1-palmitoyl-2-oleoyl-*sn*-glycero-3-phosphocholine; MGDG, monogalactosyl diglyceride; DGDG, digalactosyl diglyceride; CTAB, hexadecyltrimethylammonium bromide; T_c, main transition temperature; T_p, pretransition temperature; A, Hamaker constant (in joules); K_s, spring constant (in newtons per meter); K_a, association constant (in M^{-1}); cmc, critical micelle concentration.

0006-2960/85/0424-4608$01.50/0 © 1985 American Chemical Society

Olphen, 1977) or across stacked multibilayers (or lamellar liquid-crystalline phases) of phospholipids and phospholipid mixtures, the bilayer spacings being monitored by X-ray diffraction (Le Neveu et al., 1976, 1977; Parsegian et al., 1979). Thus, using the osmotic pressure technique on a number of different lecithins, PE, and PC + cholesterol mixtures, Lis et al. (1982a) found that the repulsive hydration forces have a range of 2–3 nm and that they decay exponentially with distance, with characteristic decay lengths ranging from 0.14 to 0.32 nm.

The third method involves meaasuring the force between two adsorbed bilayers. For this, a direct force-measuring apparatus is employed that will be briefly described in the following section. With this apparatus, the repulsive hydration forces between two CTAB bilayers adsorbed on two rigid, molecularly smooth surfaces of mica were measured (Pashley & Israelachvili, 1981; Israelachvili, 1985b) and found to be of shorter range (<2 nm) than across a free soap film (>2.5 nm). Likewise, Horn (1984) found that the hydration force between two adsorbed egg lecithin and DLPC bilayers is very similar but of somewhat shorter range than that measured between free bilayers by using the osmotic pressure method.

The literature is confusing concerning theoretical interpretations of hydration forces, and the matter is still wide open. Continuum mean-field theories of hydration forces predict an exponential force law (Marcelja & Radic, 1976; Gruen & Marcelja, 1983; Jönsson & Wennerström, 1983), whereas theoretical studies where the discrete (i.e., noncontinuum) molecular nature of the aqueous solvent is specifically taken into account predict an *oscillatory* force law between lecithin bilayers with fixed head groups (Kjellander & Marcelja, 1985). In addition, Helfrich (1978) and Sornette & Ostrowsky (1984) have noted that thermal curvature fluctuations of fluid bilayers will also give rise to a repulsive "steric" or "undulation" force that is also exponentially repulsive at large distances.

Electrostatic (Double-Layer) Forces and van der Waals Forces. Concerning the forces at longer range, beyond 2–3 nm, there are good experimental data to show that the repulsive electrostatic double-layer forces between bilayers are well described by theory: these forces have now been measured between anionic phospholipid bilayers (Cowley et al., 1978), between cationic CTAB bilayers (Pashley & Israelachvili, 1981), across soap films (Donners et al., 1977), and more recently between thylakoid membranes by using the osmotic pressure technique (Diederichs et al., 1984).

Materials and Methods

Force-Measuring Apparatus. In this paper, we report the results of a series of direct force measurements between PC and PE bilayers employing an apparatus that has been previously used to measure various forces between surfaces in liquids, e.g., van der Waals forces (Israelachvili & Adams, 1978), double-layer and hydration forces (Pashley, 1981a,b; Pashley & Israelachvili, 1984a,b; Horn, 1984), the attractive "hydrophobic interaction" (Israelachvili & Pashley, 1982, 1984), and adhesion forces (Israelachvili, 1982). The apparatus contains two curved molecularly smooth surfaces of mica (of radius $R \approx 1$ cm) facing each other, between which the interaction forces are measured directly via a variety of interchangeable force-measuring springs (Israelachvili & Pashley, 1984). In the present experiments, each mica surface has a lipid bilayer deposited on it. The procedure adopted for depositing the bilayers on the mica surfaces and mounting them into the apparatus is described by Marra (1985). The separation between the two surfaces is measured by use of an optical technique using multiple-beam interference fringes called "fringes of equal chromatic order" or FECO (Israelachvili, 1973). From the positions and shapes of the FECO fringes seen in the spectrometer, the distance between the two surfaces can be measured, often to better than 1 Å, as can the shapes of the two surfaces and the refractive index of the material between them; in particular, this allows for independent determinations of the quantity of material deposited or adsorbed on the surfaces (Pashley & Israelachvili, 1981; Israelachvili et al., 1979). Finally, from the shapes of the two initially curved surfaces, any adhesive deformations and fusion of bilayers can be directly monitored (with time) during the course of an experiment (Israelachvili et al., 1980a; Horn, 1984).

The force-measuring apparatus allows for both attractive and repulsive forces to be measured; it offers a method for measuring equilibrium force laws at constant chemical potential of the surrounding solvent medium and is particularly suitable for adhesion studies and for observation of the molecular events accompanying the fusion of two bilayers (Horn, 1984).

Preparation of Bilayer-Coated Surfaces. In these experiments, the force-measuring apparatus described above was used to measure the forces between two lipid bilayers deposited with the Langmuir–Blodgett deposition technique on two molecularly smooth substrate surfaces of mica (the mica surface is a chemically inert aluminosilicate lattice).

Monolayers of Avanti DLPC, DMPC, DPPC, DSPC, and DPPE were spread on water in the Langmuir trough from hexane–ethanol mixtures, and surface pressures were measured by the "maximum pull on a rod" method (Padday et al., 1975). The pressure–area (II–A) curves obtained were in agreement with those previously given in the literature. A series of calibration depositions were then carried out on large mica sheets to obtain the "transfer ratios" at different deposition pressures, i.e., the ratio of the area per molecule in the monolayer to that actually being deposited (transferred) onto the mica as it is slowly raised out of the water. A second series of transfer ratio calibrations was carried out for the return (downward) deposition of the second monolayer. In this way, it is possible to deposit PC or PE bilayers on mica, or a bilayer where the first monolayer is PE and the second PC, with known head-group areas. These areas were chosen to be equal to those pertaining to the phase state of the lipid bilayers in water. Full details of these preexperimental calibration procedures and depositions, giving plots of the II–A curves and transfer ratios, are described by Marra (1985).

Once a bilayer had been deposited on each mica surface (previously glued to their silica disks), these were then transferred under water in beakers from the Langmuir trough into the waiting apparatus already filled with water, the deposited bilayers remaining immersed in water throughout. This precaution is necessary since deposited or adsorbed bilayers lose their outer monolayer on being retracted from water. In order to ensure that the second monolayer did not desorb with time in the apparatus, the water in the apparatus was presaturated with a crystal of lipid for at least 12 h. The background saturation concentration of lipid monomers at the cmc (typically $>10^{-10}$ M) ensured that the bilayers did not desorb (over a period of at least 24 h) and that thermodynamic equilibrium was established between lipid monomers in solution and lipid molecules in the bilayers, as was indeed ascertained experimentally (see Results).

Results

Thickness of Adsorbed Bilayers and Operational Definition of the Bilayer–Water Interface. Before describing results of

Table I: Areas and Thicknesses of Adsorbed Bilayers

phospholipid	temp (°C)	phase state	area deposited (nm^2)	anhydrous bilayer thickness, T (nm): deposited (±0.1 nm)	anhydrous bilayer thickness, T (nm): from refractive index measurements[a] (±0.3 nm)
			Deposited		
DLPC	22	fluid	0.70	3.1	3.6
DMPC	16	pretransition	0.52	4.15	4.2
DMPC	30	fluid	0.68	3.5	3.8
DPPC	21	gel	0.52	4.6	4.6
DSPC	21	gel	0.52	5.0	5.1
DPPE	21	gel	0.42	5.3	
			Adsorbed from Solution[b]		
DLPC	20	fluid			3.6
egg PC	20	fluid			4.0

[a] $n_b = 1.464$ assumed for all lecithins (Cherry & Chapman, 1969). [b] R. G. Horn (unpublished results).

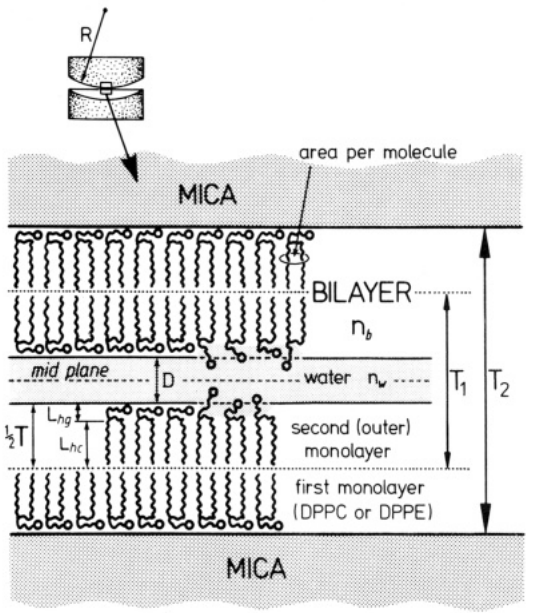

FIGURE 1: Definition of distances and refraction indices for two planar surfaces with an adsorbed or deposited bilayer on each. For two cylindrically curves surfaces of radius R at a distance D apart, the force $F(D)$ between them is related to the interaction energy per unit area $E(D)$ between two planar surfaces by $E(D) = F(D)/2\pi R$ (Derjaguin, 1934; Israelachvili, 1985a).

force measurements between bilayer surfaces at the angstrom level, it is appropriate to establish where these surfaces are. This moot point is particularly important for bilayer surfaces because, unlike solid surfaces, they are fluid and dynamically mobile—characterized by thermal undulations and fluctuations of the bilayer as a whole, the hydrocarbon–water interface, and the protruding head groups.

The configuration of the bilayers adsorbed on the two apposing mica surfaces is shown schematically in Figure 1 where we shall define the interbilayer separation—the distance between the two bilayers across water—by D, where $D = 0$ corresponds to hypothetical "contact" with no water left between the two bilayers. Of course, in practice head-group penetration into the aqueous space and the repulsive hydration forces needed to fully dehydrate them may be so large that $D = 0$ is never attained, but this does not alter the convenience of this operational definition of D, which is the same as that adopted by LeNeveu, Rand, Parsegian, Lis, and co-workers for describing interbilayer forces in multibilayer systems.

Table I shows the areas per lipid molecule deposited in the second (outer) monolayers (Figure 1) and the corresponding anhydrous bilayer thickness (T) as determined from the volumes occupied by the hydrocarbon chains and head groups. The volume of a saturated chain in the gel state is $27.4 + 26.9n$ Å^3 per n-carbon chain (Tanford, 1980), which corresponds to a density of 0.87 g/cm^3, while for chains in the fluid state a density of 0.75–0.77 g/cm^3 was used (the values for dodecane–hexadecane). The polar head-group volumes were taken as 324.5 Å^3 for PC and 243 Å^3 for PE (Small, 1967). For example, for DPPC with area = 52 Å^2, we calculate $T = 2\{[2(27.4 + 26.9 \times 15) + 324.5]/52\} = 45.6$ Å. These thicknesses are given in column 5 in Table I, where the accuracy is estimated at about ±1 Å (±0.1 nm).

As mentioned before, from measurements of the mean refractive index of the medium between the two surfaces at some particular separation, one can determine the amount of material (other than water) present between the surfaces. The only additional information needed is the tangential component of the refractive index of the adsorbed material, which in the present study is the lecithin bilayer whose refractive index will be taken as $n_b = 1.464$, the value obtained for egg PC (Cherry & Chapman, 1969). R. G. Horn (unpublished results) measured the refractive index of egg PC and DLPC bilayers after they had adsorbed onto mica surfaces from a dilute solution of vesicles. In the egg PC solution, he obtained for the total mean refractive index $n = 1.440 \pm 0.006$ at $T_2 = 9.6$ nm and $n = 1.451 \pm 0.007$ at $T_2 = 8.9$ nm (see Figure 1). The thickness of each bilayer (T) and their separation (D) are therefore given by solving $n = (2Tn_b + Dn_w)/T_2)$ and $D = T_2 - 2T$, with $n_b = 1.464$ and $n_w = 1.334$. This gives $T = 3.9$ nm at $D = 1.8$ nm and $T = 4.0$ nm at $D = 0.9$ nm, and the results for n vs. D at larger separations, up to $D = 40$ nm, were all consistent with there being two bilayers of constant thickness ~4 nm between the surfaces. Likewise, for DLPC, a value of 3.6 nm was obtained for the bilayer thickness.

In the present study, it was considered more important to measure the thickness of the outer two deposited monolayers ($^1/_2T$) (since the first monolayer was often of a different lipid such as DPPC or DPPE to ensure its stability). Accordingly, the mean refractive index was here measured across T_1 rather than T_2 (see Figure 1). The calibration of $T_1 = 0$ was more conveniently accomplished at the *end* of each experimental run by slowly draining the apparatus of liquid, which removes the second monolayer, exposing only the hydrophobic first layer, and then bringing these two monolayers into contact in air. Table I (last column) shows the results obtained for T (twice the second monolayer thicknesses, $^1/_2T$) from such measurements. The two values obtained by Horn for the bilayers adsorbed from solution are also given. Most of these readings were made at aqueous separations D in the range 1–2 nm which covered the range over which the short-range hydration forces were measured.

We note from Table I that within experimental error there

Table II: Adhesion Parameters in Pure Water

phase state	bilayer lipids	equilibrium separation, D_0 [range of hydration force (nm)]	adhesive force, F_0/R (mN/m)	adhesive energy, $E_0 = F_0/2\pi R$ (mJ/m^2)[a]	Hamaker constant,[b] A (J)
$T > T_c$	DLPC (22 °C) DMPC (30 °C)[c]	2.4–2.5	0.6 ± 0.1	0.1	$(7 \pm 1) \times 10^{-21}$
$T < T_c$	DMPC (15 °C) DPPC (21 °C) DSPC (21 °C)	2.1–2.2	0.95 ± 0.15	0.15	$(7 \pm 1) \times 10^{-21}$
	DPPE (21 °C)	1.2	5.2 ± 0.5	0.8	

[a] mJ/m^2 ≡ erg/cm^2. [b] Deduced from adhesion forces, eq 4. In high concentrations of monovalent electrolyte, the Hamaker constant is reduced (see later). [c] Same results obtained for DMPC when deposited at 30 °C or after heating from 15 °C ($T < T_c$) to 30 °C.

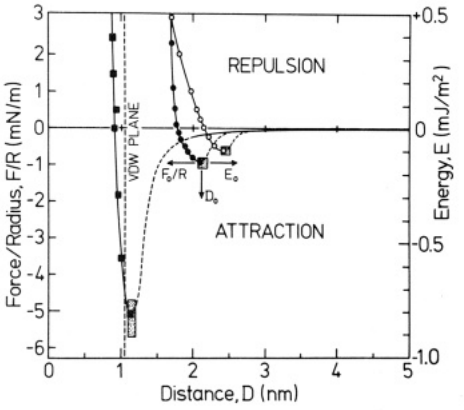

FIGURE 2: Measured force laws between adsorbed phospholipid bilayers in water around the equilibrium region. (○) Lecithins in the fluid state ($T > T_c$), DLPC at 22 °C and DMPC at 30 °C; (●) lecithins in the gel or pretransition state ($T < T_c$), DPPC and DSPC at 21 °C and DMPC at 15 °C; (■) DPPE in the gel state at 22 °C. The long-range attractive van der Waals forces beyond 2 nm were measured accurately only for DPPC and DPPE (see Figure 3). The squares around the force minima enclose the limits of error of the adhesion force F_0/R (or energy $E_0 = F_0/2\pi R$) at separation D_0.

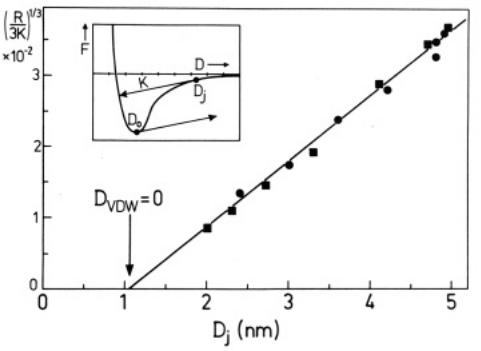

FIGURE 3: Inward jumps from D_j as a function of $(R/3K_s)^{1/3}$ where K_s is the spring stiffness (in newtons per meter) and R the surface radius (in meters): (●) DPPC; (■) DPPE.

is excellent agreement between the bilayer thickness deduced from the areas deposited and from the refractive index measurements. The slightly higher value obtained for the bilayer thicknesses of DLPC in the last column may be due to its having a higher intrinsic refractive index than that assumed (1.464), arising from the larger relative contribution of the polar head group for this short-chained lipid. We also mention that as long as the aqueous solution was saturated with lipid monomers at the cmc, the deposited bilayers remain stable with time (up to at least 24 h) and show no tendency to desorb.

Forces in Pure Water (No Electrolyte). Figure 2 shows the measured force laws for DLPC, DPPC, and DPPE at 21–22 °C. The force laws of DSPC and DMPC (at 15 °C) were practically indistinguishable from that of DPPC, while DMPC (at 30 °C) was very similar to DLPC. For the lecithins, the equilibrium separations, D_0, and adhesion forces, F_0/R, were found to fall into two distinct groups: for bilayers in the gel state ($T < T_c$), the equilibrium separations are smaller and the adhesions larger than for the fluid bilayers ($T > T_c$), while for DPPE bilayers ($T < T_c$) the equilibrium separation is *much* smaller and the adhesion *much* larger than for any of the lecithins (Table II). More significantly, we may note the general trend that the closer two curved bilayers come at equilibrium, the greater the adhesion force [or, equivalently, the adhesion energy (E_0) between two planar bilayers].

To measure the much weaker long-range attractive van der Waals forces (beyond D_0), a variable spring facility was employed (Israelachvili & Pashley, 1984), but only for DPPC and DPPE. Figure 3 shows the distances (D_j) from which the two surfaces jumped in as a function of the (variable) spring constant (K_s). The attraction is due to the van der Waals interaction; the force between two curved surfaces of radius R (Figure 1) is given by

$$F = -AR/6D^2 \quad (1)$$

where A = the nonretarded Hamaker constant. These jumps or instabilities should therefore occur when

$$K_s = dF/dD = AR/3D_j^3 \quad (2)$$

so that a plot of $(R/3K_s)^{1/3}$ against D_j should yield a straight line whose slope gives the Hamaker constant A and whose intercept gives the "van der Waals plane" from which the van der Waals force *effectively* originates. [Since the distances over which the van der Waals force was measured were less than the bilayer thickness, we expect the simple expression of eq 1 to apply (Mahanty & Ninham, 1976), though for bilayers the plane of origin of the van der Waals force may well be a diffuse one, rather than a sharp, well-defined, interface as for solid surfaces. The application of eq 1 to the results must therefore be viewed as a first approximation.] From Figure 3, we find that for both DPPC and DPPE the effective van der Waals plane is at $D = 1.05 \pm 0.10$ nm, which is shown by the vertical dashed line in Figure 2. If the van der Waals plane (where $D_{VDW} = 0$) is indeed beyond $D = 0$, it indicates that the thermal motions of the head groups must take them out by at least 0.5 nm beyond each surface; the significance and implications of this will be discussed later.

In Table II, we also give the values for the interfacial free energy per unit area, E_0, of two planar bilayers at their equilibrium separation, and the corresponding Hamaker constants (A) deduced from the adhesion forces. These quantities are related to the adhesion force F_0 by

$$E_0 = F_0/2\pi R \quad (3)$$

and

$$F_0/R \approx A/6D_{VDW}^2 \approx A/6(D_0 - 1.05\ \text{nm})^2 \quad (4)$$

For DPPE, since the adhesion at $D_0 \approx 1.2$ nm occurs so close to $D_{VDW} = 0$, it was not possible to obtain a reliable estimate

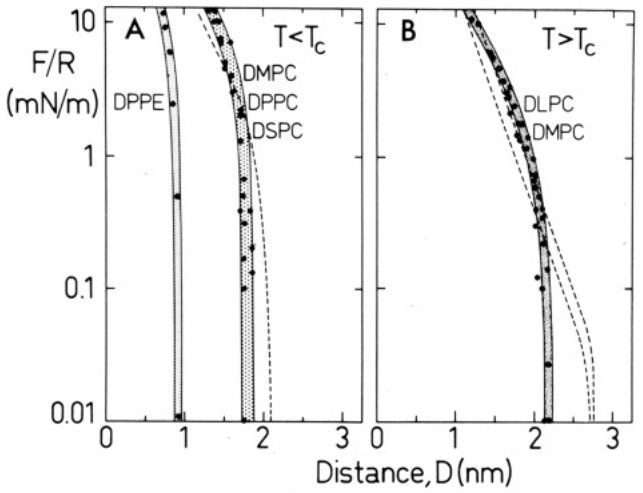

FIGURE 4: Repulsive forces at separations below equilibrium separations (continued from Figure 2). (A) Bilayers in the gel or pretransition state ($T < T_c$): DPPE, DPPC, and DSPC at 21 °C and DMPC at 15 °C [the dashed line is the corresponding result of Lis et al. (1982a) for DSPC at 25 °C]. (B) Lecithin bilayers in the fluid state ($T > T_c$): DLPC at 22 °C and DMPC at 30 °C [the dashed lines are the results of Lis et al. (1982a) for DLPC at 25 °C and DMPC at 27 °C]. At F/R values above 10 mN/m and up to 10^3 mN/m, the initially curved surfaces flatten, but the bilayers do not fuse, even at pressures up to 40 atm.

for the Hamaker constant at these small separations. Returning to Figure 3, we note that at long range the van der Waals interaction is well described by eq 1 with a Hamaker constant of $(1.3 \pm 0.2) \times 10^{-21}$ J, i.e., a factor of 5 smaller than the values deduced from the adhesion forces. Possible reasons for this "discrepancy" will be discussed under Discussion.

Figure 4 shows the measured repulsive parts of the force curves for all the lipids studied, now plotted on a log graph. The repulsive forces for DSPC, DPPC, and DMPC (at $T < T_c$) all fell within the narrow shaded band (Figure 4A) while those for DLPC and DMPC (at $T > T_c$) fell within another, slightly farther out (Figure 4B). For comparison, the previous measurements of these repulsive forces for DSPC, DLPC, and DMPC by Lis et al. (1982a) have also been added, which show [as previously found by Horn (1984) for egg PC and DLPC] that the repulsive forces between free bilayers (in lamellae) have a longer range than those between adsorbed (immobile) bilayers. This is especially true for bilayers whose lipids are in the fluid state where the equilibrium separations of the free bilayers are in the range 2.8–3.3 nm (2.8–2.9 nm for DLPC and DMPC) compared to 2.4–2.5 nm for adsorbed bilayers, while for gel-state bilayers the equilibrium separations are much the same, viz., 2.0–2.2 m for free bilayers of DPPC and DSPC compared to 2.1–2.2 nm in the present study. Closer in, however, both types of measurements appear to yield similar values for the forces [except for DPPE where both the repulsive forces, as well as the equilibrium separation of D_0 = 1.1–1.2 nm, are much smaller for the adsorbed bilayers than those measured by Lis et al. (1982a) for egg PE, where D_0 = 2.05 nm was reported]. We note that Seddon et al. (1984) obtained equilibrium spacings (D_0) in the range 0.8–1.3 nm for a variety of different PE bilayers in both the gel and fluid states, consistent with our finding.

Forces in Monovalent 1:1 Electrolyte Solutions. Since monovalent ions are believed to bind only very weakly or not at all to the neutral head groups of PC or PE, one should not expect there to be any significant repulsive double-layer force between these bilayers in the presence of salts such as NaCl. The van der Waals force, however, is expected to be reduced

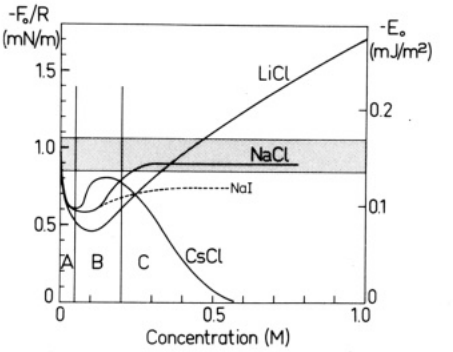

FIGURE 5: Adhesion force (F_0/R) and energy (E_0) for DPPC bilayers at 21 °C as a function of salt concentration. (Note that the direction of increasing adhesion is *upward*.) Qualitatively similar results were obtained for DLPC bilayers. The shaded band gives the range of values measured in pure water, included for comparison.

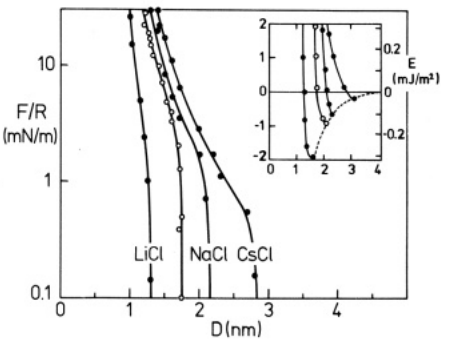

FIGURE 6: Force curves for DPPC bilayers at 21 °C in various concentrated salt solutions (see also Figure 5). From left to right, 1300 mM LiCl, pure water (reference), 150 mM NaCl, and 430 mM CsCl. No long-range double-layer forces were ever measured in water or in monovalent salt solutions with any of the lipids studied. However, at these high concentrations, some short-range repulsive double-layer force contribution due to ion binding cannot be excluded, especially in the NaCl and CsCl solutions, but is undetectable because it is swamped by the attractive van der Waals force.

in the presence of high concentrations of electrolyte, where the so-called zero frequency contribution to the Hamaker constant (3×10^{-21} J) is "screened" at distances beyond the Debye screening length (Mahanty & Ninham, 1976). Thus, if only the van der Waals force was responsible for the adhesion, we should expect decreased adhesion at increasing concentrations of electrolyte, while any ion binding should lower the adhesion even more.

Figure 5 shows results obtained for the variation of the adhesion forces (and energies) between two DPPC bilayers in the presence of various 1:1 electrolytes. Three regimes could be identified. In regime A (0–50 mM salt), the adhesion forces fell to 50–70% of the value in pure water, while in regime B (50–200 mM salt) the adhesions reached a minimum and then rose again. So far, the effects are small, and the initial decrease could be qualitatively understood for the reasons given above. However, in regime C, above 200 mM salt, the adhesion forces varied considerably depending on the electrolyte, and the results cannot now be explained by using simple concepts in terms of van der Waals and/or double-layer forces. Thus, from Figure 5 we note that in LiCl the adhesion rose dramatically (an effect that was also found with DLPC); in NaCl, it leveled off (an effect that was also found with NaI and with DLPC) while in CsCl it fell rapidly to zero. To pursue this further, full force curves were measured in concentrated solutions of LiCl, NaCl, and CsCl, shown in Figure 6. The results show that changes in the adhesion forces correlate with the equilibrium interbilayer separation D_0, viz., larger adhesions at smaller equilibrium separations (cf. Figure

Table III: Double-Layer Parameters for DPPC at 22 °C (Figure 7)

electrolyte	concn, C (mM)	surface potential, ψ_0^∞ (mV)	surface charge, σ_0^∞ C/m^2	surface charge, σ_0^∞ nm^2/Ca^{2+} bound	fraction bound, α	association constant, K_a (M^{-1})
$CaCl_2$	1.2	37	0.0048	67	0.008	118
	10.8	47	0.0190	17	0.031	114
$MgCl_2$	1.2	21	0.0028	116	0.004	20
	10.9	30	0.0118	27	0.019	19

2). It is also apparent that changes in the adhesion are due not to any increase or decrease in the attractive forces but rather to changes in the short-range repulsive forces. Thus, when eq 4 is used, the Hamaker constants estimated from the adhesion forces at the equilibrium separations do not vary much with the equilibrium separations. The only systematic correlation that was found is a slight fall in the Hamaker constants at higher electrolyte concentrations, viz., $A = (7 \pm 1) \times 10^{-21}$ in J in 0–150 mM salt, decreasing to $A = (3.5 \pm 1.5) \times 10^{-21}$ J in 1300 mM salt. We therefore note the disappearance of the zero frequency contribution of $\sim 3 \times 10^{-21}$ J in high salt, as expected theoretically.

As regards the large effects of high concentrations of electrolytes on the short-range repulsive forces, we reserve consideration of this for the Discussion; however, note here that the equilibrium aqueous separations are in the order CsCl > NaCl ≈ NaI > pure water > LiCl, which follows the hydration of the cations and which is the same order as that previously reported by Gottlieb & Eanes (1972) for the maximum uptake of concentrated solutions of these electrolytes by multilamellar lecithin bilayers.

Forces in $CaCl_2$ and $MgCl_2$ Solutions. While PC lamellae do not swell in monovalent salt solutions, they swell many hundreds of angstroms in millimolar $CaCl_2$ and $MgCl_2$ solutions due to the long-range repulsive double-layer force brought about by the binding of these ions onto the otherwise neutral surface (Inoko et al., 1975; Ohshima & Mitsui, 1978; Lis et al., 1981a,b).

Here we present results of force measurements between PC and PE in $CaCl_2$ and $MgCl_2$ solutions in the range ~1 mM to above 30 mM. In all, more than 100 force curves were measured, and it is not proposed to plot them all in detail, except in Figure 7 where the forces between DPPC bilayers in ~1 and ~10 mM $CaCl_2$ and $MgCl_2$ are shown. We note the expected longer range of the repulsive double-layer forces in the more dilute solutions, and the larger repulsions in the $CaCl_2$ solutions reflecting the stronger binding of Ca^{2+} to the phosphate group. Since the forces measured between different lipids at different salt concentrations all exhibited the same trends, we shall confine ourselves to a detailed quantitative analysis of the results in Figure 7.

When Ca^{2+} ions bind to a neutral surface such as PC, the surfaces become positively charged, and the double-layer interaction then takes place in an electrolyte where the counterion is the anion. For such systems, the surface potential (ψ_0^∞) or surface change density (σ_0^∞) of the isolated surfaces (or two surfaces at infinite separation) can be obtained by fitting the theoretical double-layer force curve to the tail end of the measured force curve (Pashley, 1981b). When this is done to the four curves in Figure 7, we obtain the potentials φ_0^∞ and charge densities σ_0^∞ shown in Table III. Note that φ_0^∞ and σ_0^∞ are related via the Grahame equation which for 2:1 electrolytes (at 22 °C) is

$$\sigma_0^\infty = \sqrt{8\epsilon\epsilon_0 kT}\sinh(e\varphi_0^\infty/2kT)(2 + e^{-e\varphi_0^\infty/kT})^{1/2}[Ca^{2+}]_\infty^{1/2} = 0.118\sinh(\varphi_0^\infty/50.9)(2 + e^{-\varphi_0^\infty/25.4})^{1/2}C^{1/2} \quad (5)$$

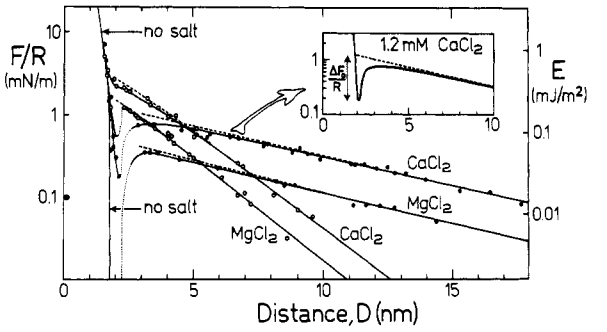

FIGURE 7: Forces between DPPC bilayers in $CaCl_2$ and $MgCl_2$ solutions at 22 °C: (●) 1.2 mM $CaCl_2$ and 1.2 mM $MgCl_2$: (○) 10.8 mM $CaCl_2$ and 10.9 mM $MgCl_2$. Dashed curves, theoretical repulsive double-layer interaction; solid curves, experimental force curves showing the effect of the van der Waals force at smaller separations. In pure water (no double-layer force), the adhesion force was $F_0/R \approx -1.0$ mN/m; the inset shows that in 1.2 mM $CaCl_2$ the dip in the repulsion ($\Delta F_0/R$) is the same, and similarly in 1.2 mM $MgCl_2$.

where φ_0^∞ is in millivolts, σ_0^∞ in Coulombs per meter squared, and the bulk electrolyte concentration C in moles per liter (or molar). Table III also shows the fraction (α) of lipid head groups that have bound a cation, calculated for an adsorption site area of 0.52 nm^2 per molecule (the head-group area per DPPC molecule).

The binding constants for the adsorptions of the cations should be described, as a first approximation, by a mass action law relating the Ca^{2+} (or Mg^{2+}) concentration at the surface, $[Ca^{2+}]_0$, to the surface density of unbound and bound sites, $[S]_0$ and $[SCa^{2+}]_0$, respectively. The equilibrium *association constant* (K_a) for the "reaction"

$$[Ca^{2+}]_0 + [S]_0 \overset{K_a}{\rightleftharpoons} [SCa^{2+}]_0$$

is therefore

$$K_a = \frac{[SCa^{2+}]_0}{[Ca^{2+}]_0[S]_0} = \frac{[SCa^{2+}]_0 e^{2e\varphi_0^\infty/kT}}{[Ca^{2+}]_\infty[S]_0} \quad (6)$$

where $[Ca^{2+}]_\infty = C$, the bulk electrolyte concentration. Since $[SCa^{2+}]_0/[S]_0 = \alpha/(1-\alpha)$, we finally have

$$K_a = \frac{\alpha e^{2e\varphi_0^\infty/kT}}{(1-\alpha)C} \quad (7)$$

which gives K_a in terms of the three measureable parameters C, φ_0^∞, and α, and which is also shown in Table III for the four curves of Figure 7. Note the constancy of the values obtained for K_a at different concentrations, for both $CaCl_2$ and $MgCl_2$.

The theoretical double-layer force curves at all separations may not be readily computed by self-consistently solving the nonlinear Poisson Boltzmann equation for each value of C, φ_0^∞, and K_a as described by Ninham & Parsegian (1971), Chan et al. (1980), and Pashley (1981b). These are shown by the dashed lines in Figure 7. These are shown by the dashed lines in Figure 7. The solid lines are the experimental force laws which include the attractive van der Waals forces, though this fitting procedure does not provide an accurate method of

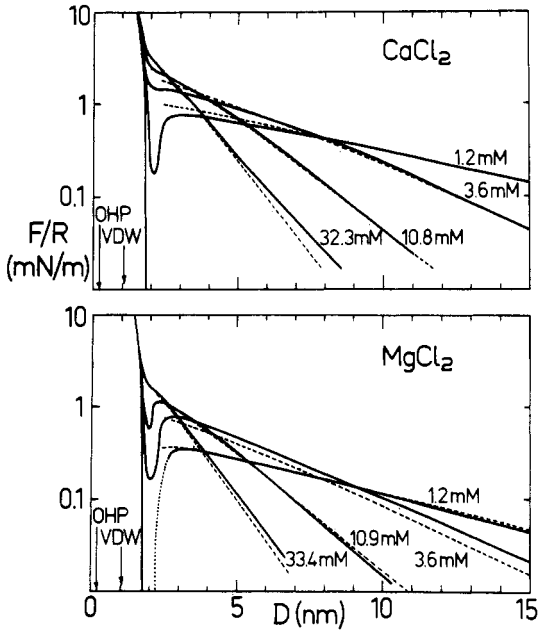

FIGURE 8: Forces between DPPC bilayers in $CaCl_2$ and $MgCl_2$ solutions at 22 °C (bilayers in the gel phase, $T < T_c$). Solid curves, experimental; dashed curves, theoretical curves based on the association constants given in Table IV, a long-range Hamaker constant of $A = 1.3 \times 10^{-21}$ J, and $D_{VDW} = 0$ at $D = 1.05$ nm. Results for DSPC were very similar.

Table IV: Double-Layer Parameters for All Phospholipids

bilayer lipid	association constant, K_a (M^{-1}) Ca^{2+}	Mg^{2+}	location of OHP[a] relative to $D = 0$ per surface (±0.1 nm)
DPPC (22 °C, gel phase)	120	20	0.1
DMPC (16 °C, pretransition phase)	46	8.6	0.2
DLPC (22 °C, liquid phase)	15	10	0.1
DPPE (21 °C, gel phase)	12	4	0.15

[a] OHP is the outer Helmholtz plane or plane of origin of diffuse double-layer charge.

obtaining the long-range Hamaker constant, especially in view of the uncertain validity of the theoretical double-layer forces at these small distances. The adhesion minima in Figure 7 were found to be at the same separations (D_0) as in pure water but *raised* from their values in pure water (i.e., in the absence of any double-layer repulsion) by just the amount of the expected double-layer force at D_0. This is illustrated in the inset of Figure 7 where the value of $\Delta F_0/R$ is practically the same as F_0/R in pure water. Clearly, the binding of the divalent cations, while affecting the electrostatic interactions between these bilayers, does not affect the short-range hydration repulsion or the intrinsic adhesion force (or energy) except by reducing it by just the amount corresponding to the double-layer force (or energy) at the equilibrium separation. The lack of any drastic effect of Ca^{2+} or Mg^{2+} binding on the strong short-range forces is understandable considering that the fraction (α) of lipids binding these ions never exceeds a few percent (Table III).

The general features of the results of Figure 7 were found to apply to all the lipids studied at all concentrations of both $CaCl_2$ and $MgCl_2$. In particular, it was found that for each lipid the surface potential, charge, and long-range double-layer interaction could be described by a single association constant over the whole range of $CaCl_2$ or $MgCl_2$ concentrations studied (see Table IV). The results are shown in Figures 8–11, where the solid and dashed lines are now the experimental and theoretical DLVO curves, respectively. At higher electrolyte concentrations, where the Debye length is short and the

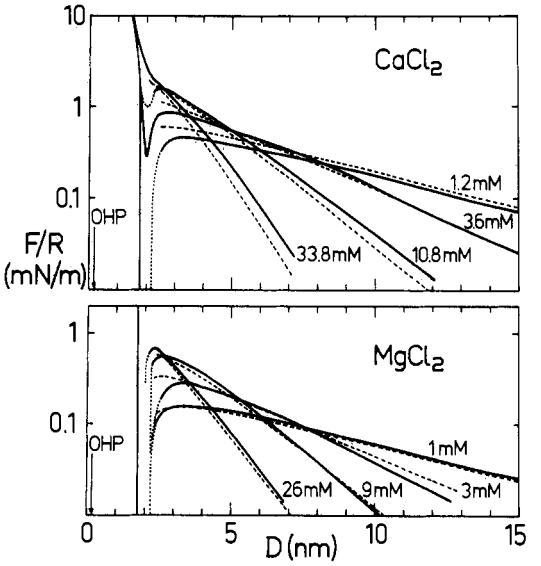

FIGURE 9: As in Figure 8 but for DMPC at $T = 16$ °C (pretransition phase, $T_p < T < T_c$).

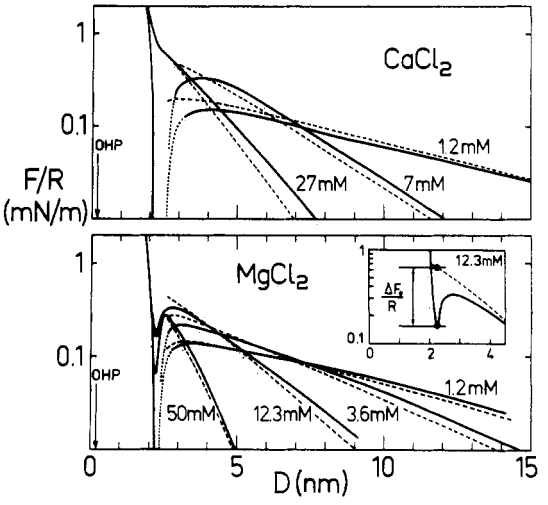

FIGURE 10: As in Figure 8 but for DLPC at 22 °C (liquid-crystalline phase, $T > T_c$). In pure water (no double-layer force), $F_0/R = -0.53$ mN/m. The inset shows the dip in the repulsion in 12.3 mM $MgCl_2$ relative to the pure double-layer force (dashed) where $\Delta F_0/R \approx 0.50$ mN/m. Likewise at 50 mM $MgCl_2$.

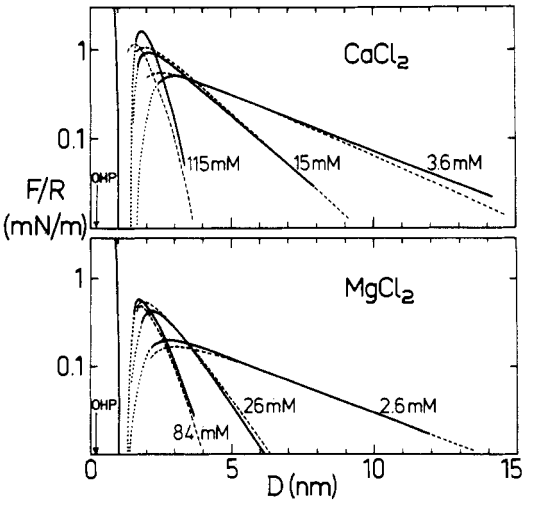

FIGURE 11: As in Figure 8 but for DPPE at 22 °C (gel phase, $T < T_c$).

double-layer forces are relatively short range, it became critical where the outer Helmholtz plane (OHP) was placed, viz., the plane of origin of the double-layer interaction. In all cases, good agreement between theory and experiment was obtained at all concentrations *with a single association constant* by placing the OHPs as indicated by the arrows in Figures 8–11 (also tabulated in Table IV). As will be discussed later, the positions of the OHPs so deduced all lie within about 0.1 nm of the negatively charged outer oxygen atoms of the phosphate groups. (Note that the theoretical curves in each figure are plotted for the same value of K_a and position of the OHP; much better agreement could, of course, be obtained if these were fitted separately for each force curve.)

Figures 8–11 cover the interactions of bilayers in their three different phase states: the gel phase (DPPC and DSPC in Figure 8 and DPPE in Figure 11), the pretransition phase (DMPC in Figure 9), and the fluid or liquid-crystalline phase (DLPC in Figure 10). They show (i) that Ca^{2+} ions always bind more strongly than Mg^{2+} ions (an effect that is more pronounced for bilayers in the gel state), (ii) that at ambient temperatures the strength of Ca^{2+} binding is in the order *gel phase* > *pretransition phase* > *liquid phase*, and (iii) that DPPE bilayers bind less than DPPC bilayers.

The dependence of Ca^{2+} binding on the phase state of DPPC and DMPC bilayers was further investigated as a function of temperature. With DMPC (main transition T_c = 24 °C) in 3.6 mM $CaCl_2$, the surface potential remained at φ_0^∞ = 33 mV at T = 14–23.5 °C (cf. Figure 9). On heating above 25 °C (and up to 30 °C), the value of φ_0^∞ gradually fell and settled at 20 mV, which is identical with that measured for DLPC in 3.6 mM $CaCl_2$ at 22 °C, i.e., in the *liquid phase* (Figure 10). The same result was obtained when DMPC was deposited at 30 °C, with a head-group area of 0.68 nm^2, and the double-layer forces then measured at 30 °C. With DPPC (pretransition temperature T_p = 35 °C) in 1.2 mM $CaCl_2$, the potential remained constant at $\varphi_0^\infty \approx$ 37 mV at 20–36 °C; then above 36 °C and up to 40 °C, it slowly fell to ~30 mV, close to that measured for DMPC in the *pretransition phase* (Figure 9). These results clearly show that the binding of divalent ions to lecithins does not depend so much on the temperature per se but on the phase state of the bilayers, and they confirm the indications of Figures 8–11 that the binding falls abruptly on going from the gel phase to the pretransition phase, and again on going from the pretransition phase to the liquid phase. The results also indicate that (at least the outer monolayers of) the deposited bilayers go through their pretransition and main transition at the same tempertures as they do in water (to within about 1 °C).

Finally, experiments were also carried out with DPPC and DLPC in 150 mM NaCl *in addition to* varying concentration of $CaCl_2$ (at 22 °C). In both systems, the surface potentials were typically well below 30 mV so that the repulsive double-layer forces were always weak and, because they were screened by the high concentration of NaCl, also of very short range. The double-layer forces could not therefore be accurately measured as a function of D. For DLPC, and $CaCl_2$ concentrations in the range 0–90 mM, the interactions were found to be determined essentially by the attractive van der Waals forces; the main effect arising from the addition of $CaCl_2$ was a small progressive reduction in the strength of the adhesion force by about 30%. With DPPC, since the Ca^{2+} binding is much greater, the effect of $CaCl_2$ on the adhesion force was more pronounced, and F_0/R fell roughly linearly from about −0.8 mN/m (in the absence of $CaCl_2$) to zero at ~10 mM $CaCl_2$.

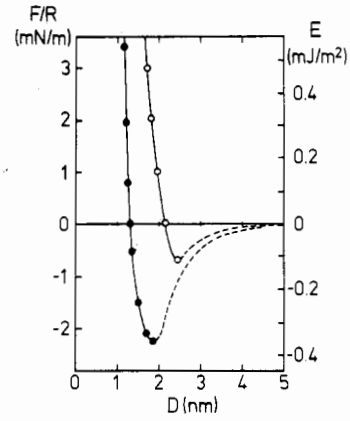

FIGURE 12: Forces between DLPC in water at 22 °C ($T > T_c$). (○) Full bilayer (as in Figure 2); (●) ~85% of full bilayer. In both cases, D = 0 refers to that of the original full bilayer.

Fusion. No fusion was observed in any of the experiments described so far. Even at the highest compressive pressures applied (exceeding 30 atm), the two initially curved surfaces simply flattened locally but did not fuse. As already mentioned, so long as the solution was fully saturated with phospholipid monomers, the deposited bilayers did not desorb. We found that in *pure water* a DLPC bilayer desorbs after about 1 h but that in a partially saturated solution desorption takes many hours (as monitored by the thinning of the bilayers with time). Clearly, as thinning progresses, the head group area (i.e., the hydrophobic area exposed to water) per lipid must increase. In one such experiment (Figure 12), after 2 h the DLPC bilayer had thinned by about 15%, since the adhesion minimum D_0 now occurred ~0.5 nm further in, and the adhesion force increased by a factor of 3. However, more importantly, the two thinned bilayers now *spontaneously* fused into one bilayer once they were brought to a separation of 1–1.5 nm, at which point the pressure between the two bilayers was still well below 4 atm (whereas for two full DLPC bilayers no fusion was observed even at pressures up to 40 atm). For a graphic illustration of the molecular events occurring during the fusion process, see Horn (1984).

Discussion

Many of the results presented in the previous section are self-explanatory and require no further discussion. Broadly speaking, the results show that there are three types of forces operating between phospholipid bilayers: at long range, we find the expected repulsive double-layer and attractive van der Waals forces while at short range, below 1–3 nm, a strongly repulsive steric hydration force balances the van der Waals attraction.

The measurements of the double-layer and van der Waals force laws have allowed us to locate the planes of origin of these two interactions which, when taken together with X-ray and neutron-scattering data, provide a consistent picture of bilayer structure as illustrated in Figure 13. Thus, the position of the outer Helmholtz plane, at $D \approx$ 0.1 nm for all the lipids, gives us the effective plane of diffuse double-layer charge and hence the likely location of cation binding. Not surprisingly, this coincides with the mean positions of the outer negative phosphate oxygens as obtained from neutron-scattering and X-ray data on electron-density profiles. For example, neutron diffraction measurements (Büldt et al., 1978) show that for DPPC the outer phosphate oxygens are 2.4 nm from the bilayer center which, from Table I, corresponds to about 0.1 nm beyond D = 0. The data of Lewis & Engelman (1983) lead to a similar result for DLPC in the fluid state.

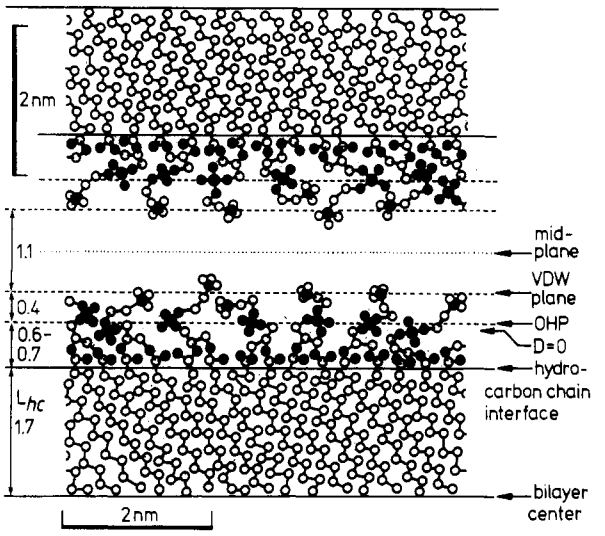

FIGURE 13: Schematic view of planar DPPC bilayer at 21 °C with various structural dimensions and interaction distances drawn to scale. The position of the OHP—the plane of charge and probable site of ion binding—coincides with the position of the PO^- group, and the plane of origin of the van der Waals interaction probably coincides with the mean position of the thermally mobile trimethylammonium groups. For different PCs and PE in different phase states, while L_{hc} will vary depending on the hydrocarbon chains, the OHP and VDW planes do not appear to change by more than 0.1 nm relative to the hydrocarbon–water interface. For free bilayers in the fluid state, additional thermal motions of the hydrocarbon–water interface could modify some of the above parameters and increase the range of the steric repulsion between bilayers.

The effective plane of origin of the van der Waals forces was also found to be at much the same distance from $D = 0$ for all the lipids, and to be located at $D \approx 0.5$ nm *per surface*. A possible explanation for this is that the head groups are not immobilized in a flat orientation on each surface but that the terminal parts of the head groups are extended *on average* by about 0.5 nm beyond the anhydrous head-group configuration (which defines $D = 0$). This is in agreement with the neutron-scattering results of D. L. Worcester (unpublished experiments), who found that the terminal (deuterated) methyl groups of fully hydrated egg lecithin bilayers sample the whole aqueous interspace during their motion, with the peak in the distribution occurring at a spacing of about 1.1 nm across the water space. Independent confirmation of this phenomenon comes from other neutron-scattering measurements of the number-density distribution of water molecules across the aqueous regions of partially and fully hydrated lecithin bilayers, which show (at a resolution of 0.7 nm and positional accuracy of 0.1 nm) that the water density nowhere attains its bulk value, even at the center of the aqueous region [see Figure 6 in Worcester & Franks (1976); Worcester, 1976].

From the adhesion force F_0 between the two cylindrically curved surfaces, each of radius R, the value of F_0/R quoted in all the results is convenient for two reasons. First, $E_0 = F_0/2\pi R$ where E_0 is the energy, or work of adhesion, per unit area of two planar surfaces. This value is also needed for calculating the total adhesion free energy of two curved deformable bilayers, e.g., two large vesicles (Israelachvili, 1985c). Second, it gives the force needed to separate a vesicle of radius $R = 1$ m from contact with a planar surface, or twice the force to separate two vesicles each of radius $R = 1$ m. For other radii, the force of adhesion simply scales by R.

The measured adhesion forces and energies ($E_0 \approx 0.1$ mJ/m^2 for PCs in water) are much higher, by a factor of about 4, than would be obtained if one assumes that the van der Waals plane is at $D = 0$. This is important for estimating interbilayer and intervesicle adhesion energies and has important implications for theoretical considerations of fusion and the relative stability of vesicles and multibilayer liposomes (Israelachvili et al., 1980b). From the adhesion forces, we have deduced that the effective Hamaker constants at short range are all within $A = (6 \pm 2) \times 10^{-21}$ J, when referred to $D_{VDW} = 0$ at $D = 1.05 \pm 0.1$ nm (Figure 13). For hydrocarbons such as hexadecane across water, we expect $A \approx (5\text{–}7) \times 10^{-21}$ J (Israelachvili, (1985a), and since the head-group region contains water, one might expect even lower values. The slightly higher values obtained could be due to the higher contributions from the polar head group and/or to some residual hydrophobic attraction (Israelachvili & Pashley, 1984) in addition to the van der Waals contribution.

At longer range, beyond the adhesive minima, the value of A is much less, viz., $A = (1.3 \pm 0.2) \times 10^{-21}$ J. It is possible that this lower value arises from the screening of the so-called temperature-dependent zero frequency contribution to A which theoretically is about 3×10^{-21} J for hydrocarbons across water (Mahanty & Ninham, 1976). This is expected to occur at large distances but only in high salt; here, the presence of high concentrations of the negative and positive charges of the zwitterionic head groups between the two surfaces may already act to reduce the Hamaker constant at distances beyond the adhesive minima. We mention that in similar measurements (Marra, 1985) of the van der Waals forces between bilayers of the completely nonionic sugar head-group lipid DGDG a long-range Hamaker constant of $A \approx 7 \times 10^{-21}$ J was obtained in water at distances up to 5 nm, which fell to $A \approx 3 \times 10^{-21}$ J in 0.2 M NaCl, as expected theoretically.

Thus, for PE and PC, while the all-important adhesion force appears to be well given by a reasonable Hamaker constant, the complete force law cannot be described by a simple power law, or a single Hamaker constant, over the whole distance regime.

Likewise, the short-range repulsive forces cannot be described by a simple equation, such as a single-exponential function. In some cases, the repulsion closer in could be fitted by an exponential function (see Figure 4 and 6), but further out, toward the equilibrium separations D_0, the repulsive forces always fall much more steeply.

There is a definite correlation between the range of the repulsive forces and the phase states of bilayers, the range being greater for bilayers in the fluid state ($T > T_c$) than in the gel state ($T < T_c$). At this point, it is worth comparing the results with the repulsive forces previously measured by using the osmotic pressure technique (see Figure 4) where the agreements are quite good, bearing in mind that the quoted distances in the two types of experiments may differ slightly (Rand and co-workers also assumed a somewhat different density for all their lipids both above and below T_c). In particular, both experiments find that the repulsive forces are of longer range for bilayers above T_c than below T_c.

As noted in the introduction, the molecular mechanism responsible for the short-range repulsion is still unclear. It cannot be simply a pure hydration force due solely to water structure effects since, as already discussed, the aqueous region is not pure water but contains the thermally mobile head groups [see also Zaccai et al. (1979)]. As proposed by Huh (1979), these must contribute their own entropic steric repulsion in the same way that surfaces with adsorbed polymers repel each other (Dolan & Edwards, 1974). Indeed, it is noteworthy that both theoretically and experimentally this type of steric repulsion is in general expected to be exponentially repulsive at short range but decaying more rapidly at larger

distances (Dolan & Edwards, 1974; Israelachvili, 1985b; Klein & Luckham, 1984). It is proposed that this type of interaction is behind the hydration forces so far measured between lipid and surfactant bilayers, where the role of the hydration shell around each head group comes into the picture in determining the excluded volume of the head groups which will extend the range of the repulsion (Dolan & Edwards, 1975). This interpretation in terms of a coupled steric hydration interaction is consistent with all the force measurements reported so far on such systems. Furthermore, it explains the increased range of these forces between free bilayers above T_c, due to the increased thermal fluctuations and undulations of the now fluid bilayers.

Clearly, the steric contribution to the total repulsion is complex and made up of at least three interactions: a (polymer-type) steric repulsion as discussed above, a contribution from long-wavelength undulations of bilayers (Helfrich, 1978; Sornette & Ostrowsky, 1984), and a contribution from local fluctuations in bilayer thickness (Lis et al., 1982b). Further insight into the relative contributions of these three interactions may be gleaned by comparing the results on adsorbed bilayers with those using the osmotic pressure technique on free bilayers (cf. Figure 4). First, we find that the range of the repulsive forces in pure water is the same for PC bilayers below T_c, with D_0 in the range 2.0–2.2 nm in both of systems. This suggests that the steric hydration interaction of the *head groups* is mainly responsible for this repulsion. For PC bilayers in the fluid state, where additional thermal thickness fluctuations and undulations of whole bilayers should be expected, the repulsion between free bilayers is now of longer range than that between adsorbed bilayers (cf. equilibrium separations D_0 in the range 2.7–3.3 nm for the free bilayers with 2.4–2.5 nm for adsorbed bilayers). Clearly, the restricted possibilities for undulations of adsorbed bilayers has reduced the range of the steric hydration repulsion compared to that for free bilayers (Israelachvilli, 1985b). Thus, above T_c, there is a significant contribution to the repulsion from all three types of steric hydration interactions.

What can we say about the relative importance of the steric and purely hydration force contributions? Can they be separated? As described earlier, the refractive index results show that there is no measurable extrusion of the bilayers as they are forced together (at least over the range of compressive forces of these experiments). Consequently, the repulsive forces reflect the *simultaneous* entropic compression and dehydration of the head groups. These two effects may be coupled so intimately as to be inseparable. It may be possible to consider the interaction as a steric one, with the hydration of the protruding hydrophilic head groups treated simply as an excluded volume effect, increasing their effective volumes above their van der Waals radii (Dolan & Edwards, 1975). It is also possible that the fundamental hydration interaction is oscillatory (Pashley & Israelachvili, 1984b) but that the inherent roughness of bilayer surfaces and the thermal motions of the head groups and hydrocarbon–water interfaces smear these out and extend the range of the interaction (D. Sornette and N. Ostrowsky, unpublished results) so that there remains only a smooth overall repulsive force.

Further insight into the hydration force contribution comes from the effects of high concentrations of LiCl, NaCl, and CsCl. The reduced range of the steric hydration force in 1.3 M LiCl may be due to a "salting-out" effect, whereby the highly hydrated Li^+ ion now competes with the head groups for water. The reverse occurs with the very weakly hydrated Cs^+ ion, while Na^+ is intermediate, giving a hydration force and adhesion similar to that in pure water. We also conclude that there is no significant binding of monovalent ions to PC and PE bilayers (unless both the anions and cations bind equally).

With $CaCl_2$ and $MgCl_2$ solutions, significantly cation binding already occurs below 1 mM. This results in a long-range double-layer repulsion but does not affect the short-range steric hydration repulsion. For any particular lipid system, a single binding constant or "association constant" is enough to describe quantitatively the bindings at all electrolyte concentrations from 1 to 100 mM, and the repulsive double-layer forces are also excellently described by theory. At shorter range, the van der Waals forces cause the surfaces to jump into adhesive contact, but the Hamaker constants deduced from these inward jumps could not be calculated as accurately as in pure water (i.e., in the absence of double-layer forces). However, a range of A values from 1.5×10^{-21} to 6×10^{-21} J would account for all the data near the force maxima, which we note is intermediate between the value obtained from the equilibrium adhesion forces closer in and the longer range value measured in pure water.

As in many colloidal and biocolloidal systems, the binding of Ca^{2+} was always greater (by up to a factor of 2) than that of Mg^{2+}, a consequence, no doubt, of the lower hydration of Ca^{2+}. Both bindings (especially that of Ca^{2+}) were also sensitive to the phase states of PC bilayers, in the order gel state > pretransition state > liquid state. These trends are entirely consistent with those previously reported by Lau et al. (1980) and Lis et al. (1981a). The binding constants we have measured for Ca^{2+} and Mg^{2+} to DPPC and DMPC in the absence of NaCl (Table IV) are about a factor of 2 larger than those measured by MacDonald and McLaughlin by electrophoresis (personal communication). Concerning calcium binding to bilayers in the fluid state, our value of $K_a \approx 15\ M^{-1}$ for Ca^{2+} binding to DLPC is very close to that of $K_a \approx 19\ M^{-1}$ measured by Akutsu & Seelig (1981) for DPPC at 59 °C using deuterium magnetic resonance, while in a later study with POPC at 40 °C (Altenbach & Seelig, 1984; Table I) the binding measured in dilute $CaCl_2$ solutions was again very similar.

Finally, the fusion of two bilayers was observed only once they were about 15% thinner than their equilibrium thickness, i.e., exposing a larger hydrophobic area than when in the natural state. Fusion is initiated at one point via a local deformation involving the parting of head groups followed by a breakthrough and meeting up of the hydrocarbon chains of apposing bilayers, as described by Horn (1984) and earlier suggested by Hui et al. (1981). Interesting, the *shape* of the force law between the two thinned bilayers at distances down to the point of fusion was not obviously different from some of the other force laws measured when there was no fusion: the long-range attraction and adhesion were greater than for unthinned bilayers, perhaps due to some additional hydrophobic interaction, and the repulsive wall was less steep, perhaps due to the weakened, softer bilayers. While more work needs to be done in this area, it does appear that a knowledge of the interbilayer force law alone does not allow us to deduce when fusion will occur. The *intra*bilayer forces involved in the local stresses and deformations accompanying the fusion process must also be considered.

ACKNOWLEDGMENTS

We are grateful to Richard M. Pashley for writing the computer program for computing the theoretical double-layer forces (with charge regulation) and to Roger Horn for providing us with his refractive index data on egg PC and DLPC bilayers. We also thank the following for their constructive

comments: David Gruen, Stuart McLaughlin, Roger Horn, Stjepan Marcelja, Hugo Christenson, and Didier Sornette.

Registry No. DLPC, 18285-71-7; DMPC, 13699-48-4; DPPC, 2644-64-6; DSPC, 4539-70-2; DPPE, 3026-45-7; Ca, 7440-70-2; Mg, 7439-95-4; LiCl, 7447-41-8; NaCl, 7647-14-5; NaI, 7681-82-5; CsCl, 7647-17-8; $CaCl_2$, 10043-52-4; $MgCl_2$, 7786-30-3.

REFERENCES

Akutsu, H., & Seelig, J. (1981) *Biochemistry 20*, 7366.

Altenbach, C., & Seelig, J. (1984) *Biochemistry 23*, 3913.

Büldt, G., Gally, H. U., Seelig, A., Seelig, J., & Zaccai, G. (1978) *Nature (London) 271*, 182.

Chan, D. Y. C., Pashley, R. M., & White, L. R. (1980) *J. Colloid Interface Sci. 77*, 283.

Cherry, R. J., & Chapman, D. (1969) *J. Mol. Biol. 40*, 19.

Clunie, J. S., Goodman, J. F., & Symons, P. C. (1967) *Nature (London) 216*, 1203.

Cowley, A. C., Fuller, N. L., Rand, R. P., & Parsegian, V. A. (1978) *Biochemistry 17*, 3163.

Derjaguin, B. V. (1934) *Kolloid-Z. 69*, 155.

Diederichs, K., Welte, W., & Kreutz, W. (1984) *8th International Biophysics Congress*, Poster 226, Bristol, U.K.

Dolan, A. K., & Edwards, S. F. (1974) *Proc. R. Soc. London, A 337*, 509.

Dolan, A. K., & Edwards, S. F. (1975) *Proc. R. Soc. London, A 343*, 427.

Donners, W. A. B., Rijnbout, J. B., & Vrij, A. (1977) *J. Colloid Interface Sci. 61*, 249.

Gottlieb, M. H., & Eanes, E. D. (1972) *Biophys. J. 12*, 1533.

Gruen, D. W. R., & Marcelja, S. (1983) *J. Chem. Soc., Faraday Trans. 2 79*, 225.

Helfrich, W.(1978) *Z. Naturforsch., A: Phys., Phys. Chem., Kosmophys. 33A*, 305.

Horn, R. G. (1984) *Biochim. Biophys. Acta 778*, 224.

Huh, C. (1979) *J. Colloid Interface Sci. 71*, 408.

Hui, S. W., Stewart, T. P., Boni, L. T., & Yeagle, P. L. (1981) *Science (Washington, D.C.) 212*, 921.

Inoko, Y., Yamaguchi, T., Furuya, K., & Mitsui, T. (1975) *Biochim. Biophys. Acta 413*, 24.

Israelachvili, J. N. (1973) *J. Colloid Interface Sci. 44*, 259.

Israelachvili, J. N. (1982) *Adv. Colloid Interface Sci. 16*, 31.

Israelachvili, J. N. (1985a) *Intermolecular and Surface Forces*, Academic Press, New York.

Israelachvili, J. N. (1985b) *Chem. Scr.* (in press).

Israelachvili, J. N. (1985c) in *Physics of Amphiphiles, Micelles, Vesicles and Microemulsions* (Degiorgio, V., & Corti, M., Eds.) North-Holland, Amsterdam.

Israelachvili, J. N., & Adams, G. E. (1978) *J. Chem. Soc., Faraday Trans. 1 74*, 975.

Israelachvili, J. N., & Pashley, R. M. (1982) *Nature (London) 300*, 341.

Israelachvili, J. N., & Pashley, R. M. (1984) *J. Colloid Interface Sci. 98*, 500.

Israelachvili, J. N., Tandon, R. K., & White, L. R. (1979) *Nature (London) 277*, 120.

Israelachvili, J. N., Perez, E., & Tandon, R. K. (1980a) *J. Colloid Interface Sci. 78*, 260.

Israelachvili, J. N., Marcelja, S., & Horn, R. G. (1980b) *Q. Rev. Biophys. 13*, 121.

Jönsson, B., & Wennerström, H. (1983) *J. Chem. Soc., Faraday Trans. 2 79*, 19.

Kjellander, R., & Marcelja, S. (1985) *Chem. Scr.* (in press).

Klein, J., & Luckham, P. F. (1984) *Macromolecules 17*, 1041.

Lau, A. L. Y., McLaughlin, A. C., MacDonald, R. C., & McLaughlin, S. G. A. (1980) *Adv. Chem. Ser. No. 188*, 50–56.

LeNeveu, D. M., Rand, R. P., & Parsegian, V. A. (1976) *Nature (London) 259*, 601.

LeNeveu, D. M., Rand, R. P., Parsegian, V. A., & Gingell, D. (1977) *Biophys. J. 18*, 209.

Lewis, B. A., & Engelman, D. M. (1983) *J. Mol. Biol. 166*, 211.

Lis, L. J., Parsegian, V. A., & Rand, R. P. (1981a) *Biochemistry 20*, 1761.

Lis, L. J., Lis, W. T., Parsegian, V. A., & Rand, R. P. (1981b) *Biochemistry 20*, 1771.

Lis, L. J., McAlister, M., Fuller, N., Rand, R. P., & Parsegian, V. A. (1982a) *Biophys. J. 37*, 657.

Lis, L. J., McAlister, M., Fuller, N., Rand, R. P., & Parsegian, V. A. (1982b) *Biophys. J. 37*, 667.

Lyklema, J., & Mysels, K. J. (1965) *J. Am. Chem. Soc. 87*, 2539.

Mahanty, J., & Ninham, B. W. (1976) *Dispersion Forces*, pp 201–202, Academic Press, London and New York.

Marcelja, S., & Radic, N. (1976) *Chem. Phys. Lett. 42*, 129.

Marra, J. (1985) *J. Colloid Interface Sci.* (in press).

Ninham, B. W., & Parsegian, V. A. (1971) *J. Theor. Biol. 31*, 405.

Ohshima, H., & Mitsui, T. (1978) *J. Colloid Interface Sci. 63*, 525.

Padday, J. F., Pitt, A. R., & Pashley, R. M. (1975) *J. Chem. Soc., Faraday Trans. 1 71*, 1919.

Parsegian, V. A., Fuller, N., & Rand, R. P. (1979) *Proc. Natl. Acad. Sci. U.S.A. 76*, 2750.

Pashley, R. M. (1981a) *J. Colloid Interface Sci. 80*, 153.

Pashley, R. M. (1981b) *J. Colloid Interface Sci. 83*, 531.

Pashley, R. M., & Israelachvili, J. N. (1981) *Colloids Surf. 2*, 169.

Pashley, R. M., & Israelachvili, J. N. (1984a) *J. Colloid Interface Sci. 97*, 446.

Pashley, R. M., & Israelachvili, J. N. (1984b) *J. Colloid Interface Sci. 101*, 511.

Seddon, J. M., Cevc, G., Kaye, R. D., & Marsh, D. (1984) *Biochemistry 23*, 2634.

Small, D. M. (1967) *J. Lipid Res. 8*, 551.

Sornette, D., & Ostrowsky, N. (1984) *J. Phys. (Paris) 45*, 265.

Tanford, C. (1980) *The Hydrophobic Effect*, 2nd ed., Wiley, New York.

Van Olphen, H. (1977) *Clay Colloid Chemistry*, Chapter 10, Wiley-Interscience, New York.

Verwey, E. J. W., & Overbeek, J. Th. G. (1948) *Theory of the Stability of Lyophobic Colloids*, Elsevier, Amsterdam.

Worcester, D. L. (1976) in *Biological Membranes* (Chapman, D., & Wallach, D. F. H., Eds.) Vol. 3, pp 1–46, Academic Press, London.

Worcester, D. L., & Franks, N. P. (1976) *J. Mol. Biol. 100*, 359.

Zaccai, G., Büldt, G., Seelig, A., & Seelig, J. (1979) *J. Mol. Biol. 134*, 693.